MS-I

CONTRACT: NAS 8-11811

QUARTERLY REPORT (II)
January 1965

N65 17515

(ACCESSION NUMBER) (THRU)

30 1

(PAGES) (CODE)

CR 60848 11

(NASA CR OR TMX OR AD NUMBER) (CATEGORY)

FACILITY FORM 602

DESIGN, DEVELOPMENT, MANUFACTURE, AND DELIVER NEW CONCEPTS FOR HIGH ENERGY RATE FORMING SYSTEM

GPO PRICE $ ______

OTS PRICE(S) $ ______

Hard copy (HC) 2.00

Microfiche (MF) .50

B. Leftheris

Republic Aviation Corporation
Manufacturing Research Department

RAC 2788

A theoretical analysis of the "Pancake" electromagnetic wave generator is presented. The results of one example are compared with test results. A 12" coil was built and tested to 58,000 joules. The coupling between the pancake coil and the driver plate was good. Pressures of 7900 psi were generated.

CONTRACT: NAS 8-11811

QUARTERLY REPORT (II)
January 1965

DESIGN, DEVELOPMENT, MANUFACTURE, AND DELIVER NEW CONCEPTS FOR HIGH ENERGY RATE FORMING SYSTEM

B. Leftheris

Republic Aviation Corporation
Manufacturing Research Department

RAC 2788

A theoretical analysis of the "Pancake" electromagnetic wave generator is presented. The results of one example are compared with test results. A 12" coil was built and tested to 58,000 joules. The coupling between the pancake coil and the driver plate was good. Pressures of 7900 psi were generated.

Republic Aviation Corporation
Farmingdale, New York

Design, Development, Manufacture, and Deliver New Concepts for High Energy Rate Forming System

Contract No. NAS 8-11811
Quarterly Report No. II

Prepared by: Basil Leftheris
Basil Leftheris
Pr. Mfg. Rsch. Engr.

Approved: J. Christiana
J. Christiana
Mfg. Rsch. Grp. Engr.

Approved: G. Pfanner
G. Pfanner, Section Head
Manufacturing Research Dept.

This report was prepared by Republic Aviation Corporation under NAS 8-11811 for the George C. Marshall Space Flight Center, National Aeronautics and Space Administration. The work was administered by the George C. Marshall Space Flight Center.

TABLE OF CONTENTS

ILLUSTRATIONS

LIST OF SYMBOLS

i – Electrical current density

μ – Electrical permeability

B – Magnetic induction

F – Force

z – vertical distance

B_x – magnetic induction in the x direction

E – Electric intensity

t – time

ρ – resistivity

V – velocity

V_z – velocity in the vertical direction

I – Electrical current

V – Capacitor voltage before discharge

X_L – Inductive reactance

R – Electrical resistance

L – inductance

Φ – magnetic flux

r – average coil radius

ρ_w – water density

C_w – water acoustic speed

A_p – driver plate cross-sectional area

m_p – driver plate mass

1.0 Introduction

The magnetic hammer principle has been established and used successfully. Some theoretical considerations were given [(1),(2)] and the problem has been generally related to magnetic forming.

One of the methods suggested was the following: A "pancake" magnetic coil is placed over a thin aluminum driver plate; with the discharge of high energy current through the coil (10, 20, 50 K joules) the driver plate is repulsed away from the coil at a high rate of acceleration. If the whole assembly was immersed in liquid (i.e. water), and a tube was placed so that the driver plate is guided, a pressure wave is generated in the water. If, in addition, a thin aluminum blank (i.e. 1/16" thick) with a die was placed under the guiding tube, the pressure wave, propagating along the tube, will hit and form it.

In this report, an attempt is made to formulate the principle and, with some reasonable assumptions, find relationships between the various parameters.

An example is presented to illustrate the analysis and the results are compared with the tests performed with such a device.

2.0 Theoretical Aspects

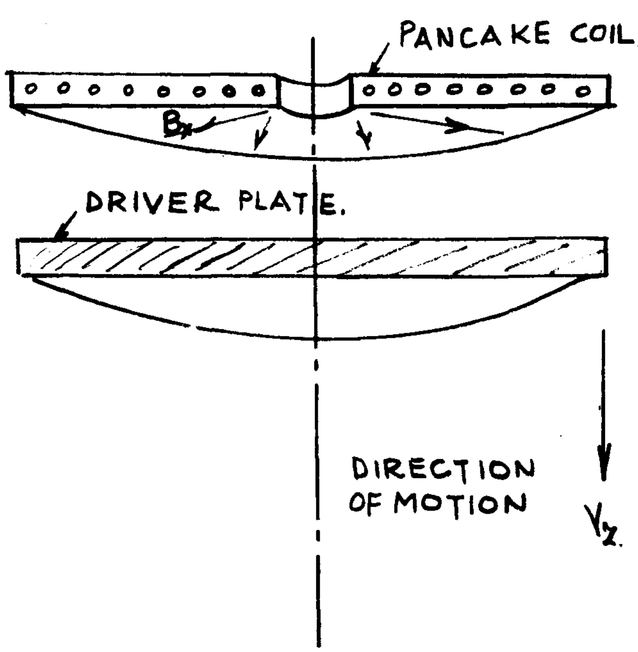

Consider the pancake coil as shown in the adjacent figure, and the driver plate shown in motion under the influence of the magnetic force.

Initially, the driver is placed in contact with the coil with only the insulation (0.02-0.05 thick) placed between them. The coil is connected to a capacitor bank which is used as the source of energy. The operation begins with the capacitor bank discharging through

1. Birdsall, D.H., Ford, F.C., Furth, H.P., Riley, R.E., Magnetic Forming, Am. Mach. Vol. 105, No. 6 p.p. 117-121
2. Furth, H.P. Waniek, R.W., Am. Mach., Jan. 22, 1962

the coil. Since inherently the current changes with time, the magnetic flux engulfing the aluminum driver plate also changes with time. This change induces a voltage in the aluminum plate and thereby a flow of current according to the aluminum resistivity.

The direction of the flow of current is opposite to the flow of current in the coil. Thus we have a current carrying conductor in a magnetic field. The conductor therefore is driven away from the coil in accordance with the "left hand" rule of electricity

The current in the aluminum is given by:

$$i = \frac{1}{\mu} \nabla \times B \quad . \quad . \quad . \quad . \quad . \quad . \quad . \qquad (1)$$

The force exerted on the driver is given by:

$$F = i \times B \quad . \quad . \quad . \quad . \quad . \quad . \qquad (2)$$

If we consider the coil lying in the xy direction then we obtain the following:

$$F_z = -\frac{1}{2\mu} \frac{\partial (B_x^2)}{\partial z} \quad . \quad . \quad . \quad . \qquad (3)$$

where the force is given in lb/ft^3.

It is now postulated that the penetration(s) of the magnetic field in the aluminum plate is <u>very small</u>: the validity of this postulation will be discussed later.

For anyone instant of time, therefore, we have from eq. (3)

$$\int_0^s F_z \, dz = \frac{B_x^2}{2\mu} = \text{pressure exerted on the}$$

surface of the driver plate; s= thickness of field penetration.

N.B. The minus sign in equation (3) means that as $\frac{\partial B_x}{\partial z}$ increases as F decreases.

Now, the electric density in the plate is due to two effects: a) voltage induced by the change of the magnetic field with time and b) voltage induced by the movement of the conductor.

Hence

$$E_{total} = E + V \times B \quad . \quad . \quad . \quad . \tag{4}$$

we also have from the general theory of electromagnetism the following equations:

$$\nabla \times E = -\frac{\partial B}{\partial t} \quad . \quad . \quad . \quad . \tag{5}$$

and $E_t = \rho \cdot i$

Hence: $E = E_t - V \times B$

$$= \rho \cdot i - V \times B$$

$$= \frac{\rho}{\mu} \nabla \times B - V \times B \quad . \quad . \quad . \quad . \quad . \quad . \tag{6}$$

$$\nabla \times E = \frac{1}{\mu} \nabla \times (\rho \nabla \times B) - \nabla \times (V \times B) \quad . \tag{7}$$

Substituting from (5) we obtain

$$\frac{\partial B}{\partial t} = \frac{1}{\mu} \nabla \times (\rho \nabla \times B) - \nabla \times (V \times B) \quad . \tag{8}$$

Equation (8) can be simplified by considering the coil in the x y plane and motion in the z plane.

Thus eq. (8) becomes:

$$\frac{\partial B_x}{\partial t} = -\frac{1}{\mu} \frac{\partial}{\partial z} \rho \left(\frac{\partial B_x}{\partial z} \right) - \frac{\partial}{\partial z} (V_z B_x) \quad . \tag{9}$$

Now multiply eq. (9) by $\frac{B_x}{\mu}$; thus

$$\frac{\partial\left(\frac{B_x^2}{2\mu}\right)}{\partial t} = -\frac{\rho}{\mu}\left(\frac{B_x}{\mu}\right)\frac{\partial}{\partial z}\left(\frac{\partial}{\partial z}B_x\right) - \frac{B_x}{\mu}\frac{\partial}{\partial z}(V_x B_x)$$

or

$$\frac{\partial\left(\frac{B_x^2}{2\mu}\right)}{\partial t} = -\frac{\rho}{\mu}\frac{\partial}{\partial z}\left[\frac{\partial}{\partial z}\left(\frac{B_x^2}{2\mu}\right)\right] + \rho i^2 - \frac{B_x^2}{\mu}\frac{\partial V_x}{\partial z} - V_x\frac{\partial\left(\frac{B_x^2}{2\mu}\right)}{\partial z} \quad (10)$$

The quantity $\frac{\rho}{\mu}$ represents the penetration velocity coeficient (3) (i.e. $h^2 = \frac{\rho}{\mu}$ where h is the penetration coefficient in $\frac{cm}{sec^{1/2}}$; for aluminum, h = 5.6 in/sec$^{1/2}$; hence if the pulse duration is 10^{-5} sec, the penetration distance is 0.0175 in.)

It is possible now to integrate equation (10) to obtain the following

$$\frac{\partial}{\partial t}\int\left(\frac{B_x^2}{2\mu}\right)dz = \int\rho i^2 - \int\frac{B_x^2}{\mu}\frac{\partial V_x}{\partial z}dz - \int V_x\frac{\partial\left(\frac{B_x^2}{2\mu}\right)}{\partial z}dz. \quad (11)$$

N. B. The term $\frac{\partial}{\partial z}\left[\frac{\partial}{\partial z}\left(\frac{B_x^2}{2\mu}\right)\right]$ is neglected on the basis that the force $\frac{\partial}{\partial z}\left(\frac{B_x^2}{2\mu}\right)$ acts only on the surface of the driver; therefore, there is no change of force with respect to distance.

If the driver plate is thin, the first impact on its surface adjacent to the coil will propagate through its thickness at the propagation velocity of the driver.

For aluminum, C=220,000 in/sec; if the plate is 1 inch thick, the wave front will traverse the thickness in 4.5 μ sec.

Hence, if the duration of the first half cycle (useful time) is in the order of 40 μ sec, the wave front will traverse the thickness of the plate nine (9) times. Each time the front traverses the thickness of the driver

(3) Diffusion of Electric Current into Rods, Tubes and Flat Surfaces, K. W. Miller, AIEE Vol. 66, 1947 p.p. 1496-1502

the velocity between the two surfaces equalizes. Thus, it is assumed that the velocity across the plate thickness is constant and that V_z represents the plate velocity: Therefore, the energy dissipated in $\left(\frac{B_x^2}{2\mu}\right)\frac{\partial V_z}{\partial z}$ is negligible.

Furthermore, since the duration of the first half cycle is small, loss due to "current heating" is negligible

Thus $\int \rho i^2 dz$ can be neglected.

Hence equation (11) can now be written as follows:

$$\frac{\partial}{\partial t}\int\left(\frac{B_x^2}{2\mu}\right)dz \cong -\int V_z \frac{\partial\left(\frac{B_x^2}{2\mu}\right)}{\partial z} dz. \qquad (12)$$

Equation (12) shows that the rate of change of the magnetic energy is equal to the rate of change of work done in moving the driver plate along the axis z . Good coupling therefore can be expected.

3.0 Electrical Aspects

In an L. C. R. circuit, the following equations are valid:

For an oscillatory condition with damping*:

$$I = \frac{V_o}{\omega_s X_L} e^{-\frac{R}{2L}t} \sin \omega_s t \quad . \quad . \quad . \qquad (13)$$

and $$\omega_s = \sqrt{\frac{1}{CL} - \frac{R^2}{4L^2}} \quad . \quad . \quad . \qquad (14)$$

For an over-damped condition*:

$$I = \frac{V_o}{\omega_s' X_L} e^{-\frac{R}{2L}t} \sinh \omega_s' t \quad . \quad . \quad . \qquad (15)$$

and $$\omega_s' = \sqrt{\frac{R^2}{4L^2} - \frac{1}{CL}} \qquad (16)$$

Equation (13) can be shown graphically as follows:

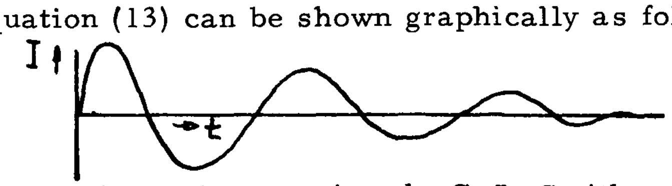

*See electricity and magnetism by C. J. Smith.

Equation (9) on the other hand varies as follows:

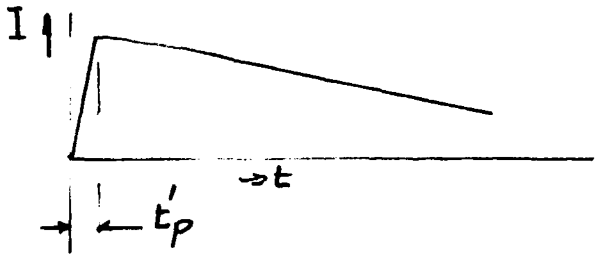

The time required to reach peak current in the over-damped condition is given by:

$$t_p' = \frac{1}{\omega_s'} \tan^{-1} \frac{2L\omega_s'}{R} \quad . \quad . \quad (17)$$

For the highly over-damped condition $\left(\frac{R}{2L} \gg \frac{1}{CL}\right)$

t_p' is approximately equal to $\frac{1}{\omega_s'}$.

For slightly over-damped $\left(\frac{R}{2L} < \frac{1}{CL}\right)$ and highly damped systems the time to reach maximum current is the same. In the tests that were carried out this time was between 50 - 100 μsec.

It is generally known that the induced voltage is given by:

$$V = -N \frac{d\Phi}{dt}$$

where Φ = magnetic flux

and N = N of turns

For a two turn secondary coil we have:

$$V = -2 \frac{d\Phi}{dt} \quad . \quad . \quad . \quad . \quad (19)$$

The value of Φ is given by:

$$\Phi = \int_{z_0}^{z} B_x 2\pi r \, dz \quad . \quad . \quad . \quad (20)$$

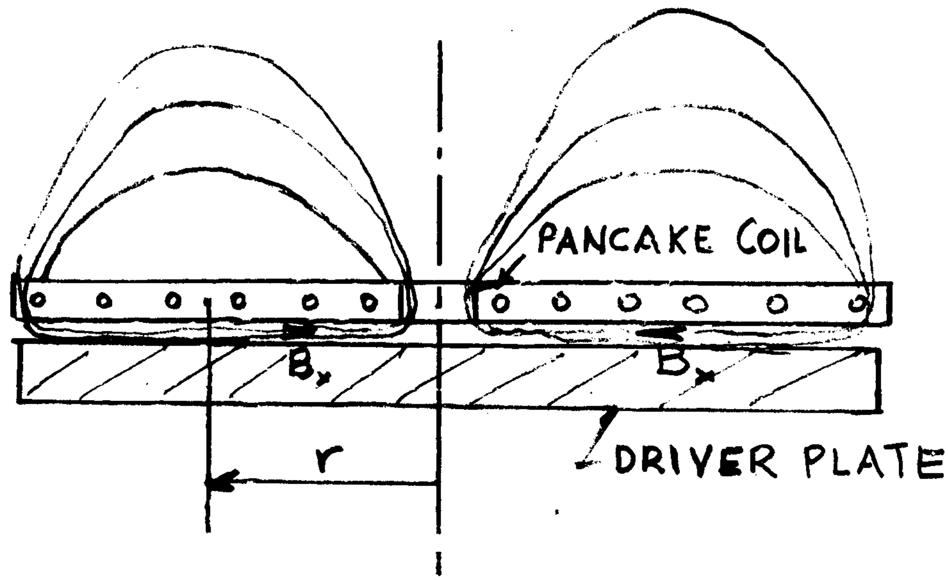

The magnetic density component B_x for a pancake coil is given by:

$$B_x = \frac{\mu I}{\pi}\left[\frac{1}{2z} + \frac{2nz}{W^2}\right] \qquad (21)$$

where I - current

z - vertical distance from the coil

n - number of turns

W width of the coil annulus

Since $z \ll W^2$, eq. (21) can be written as follows:

$$B_x = \frac{\mu I}{2\pi z} \qquad (22)$$

Hence

$$\phi = \int_{z_0}^{z} B_x\, 2\pi r\, dz \doteq \mu I r \int_{z_0}^{z} \frac{dz}{z} = \mu I r \ln \frac{z}{z_0} \qquad (23)$$

Substituting in eq. (21) we obtain:

$$V = -2\frac{d\phi}{dt} = -2\mu \frac{Ir}{\bar{z}}\frac{d\bar{z}}{dt} - 2\mu r \ln \bar{z} \frac{dI}{dt} \quad . \quad . \quad (24)$$

where $\bar{z} = \frac{z}{z_0}$, and r = average radius of the coil

It is easily deduced from equation (24) that:

$$\left.\begin{array}{l} R_2 = 2\mu r \, d \ln \bar{z} \\ \text{and } L_2 = 2\mu r \ln \bar{z} \end{array}\right\} \quad . \quad . \quad . \quad . \quad (25)$$

From equation (12) we write the following equation:

$$\frac{\partial}{\partial t}\left(\frac{B_x^2}{2\mu}\right) = -V_z \frac{\partial}{\partial z}\left(\frac{B_x^2}{2\mu}\right) \quad . \quad . \quad . \quad (26)$$

Re-writing eq. (22) we have;

$$\frac{B_x^2}{2\mu} = \frac{\mu I^2}{8\pi^2 z^2} \quad . \quad . \quad . \quad . \quad (27)$$

Hence, combining eq. (26) and (27) we obtain:

$$\mu \frac{I}{8\pi^2 z^2}\frac{dI}{dt} = 2 \frac{V_z \mu I^2}{8\pi^2 z^3}$$

(Note that I is only a function of time.)

Thus $\quad \frac{dI}{dt} = \frac{2 V_z I}{z} \quad . \quad . \quad . \quad (28)$

integrating and observing that $I = I_{max}$ when $z = z_{max}$ we obtain the following:

$$I = I_m \left(\frac{z}{z_{max}}\right)^2 \quad \text{or} \left(\frac{z}{z_{max}}\right)^2 = \frac{I}{I_{max}} \quad . \quad , \quad (29)$$

Equation (29) shows that as long as $\frac{dI}{dt}$ is positive $\frac{dz}{dt}$ is positive; at $\frac{dI}{dt} = 0$ the magnetic force is either not effective or it attracts the driver plate. At this point, the plate will begin decelerating under the force $\rho_w C_w A_p V$, starting with the initial conditions $V = V_{max}$ at $z = z_{max}$.

The short duration of the pressure wave can be seen in Figure's 1, 2. This record was taken during operation of the electromagnetic transducer.

4.0 Equation of Motion

It is now possible to write the equation of motion for the driver plate. From Newton's first law we have: $\Delta F = m \frac{dV}{dt}$

where ΔF = summation of forces acting on driver plate

m = mass of driver plate

V = driver plate velocity

t = time

It was stated earlier that the driver plate is thin and therefore any force acting on its top surface will transmit without gradients across to the surface below. The force acting on the top is given by:

$$\left(\frac{A_p B_x^2}{2\mu}\right) = \frac{\mu A_p I^2}{8\pi^2 z^2} \qquad (30)$$

where A_p = driver plate area

The water which is in contact with the lower surface (see diagram of apparatus) will react with a force:

$$F_R = \rho_w C_w A_p V \qquad (31)$$

(momentum equation of pressure wave $P = \rho \cdot c \cdot V$.)

Thus the equation of motion is:

$$m_p \frac{dV}{dt} = \frac{\mu A_p I^2}{8\pi^2 z^2} - \rho_w C_w A_p V$$

$$\text{or} \quad \frac{dV}{dt} + \frac{\rho_w C_w A_p}{m_p} V = \frac{\mu A_p I^2}{8\pi^2 m_p Z^2} \quad . \quad . \quad (32)$$

Now, when the system (capacitor bank, triggering switch, leads, coil, etc., is underdamped, eq. (24) can be written as follows:

$$\frac{dV}{dt} + \alpha V = \beta \frac{e^{-\frac{R}{L}t}}{Z^2} \sin^2 \omega_1 t \quad . \quad . \quad . \quad (33)$$

where $\alpha = \frac{\rho_w C_w A_p}{m_p}$ and $\beta = \frac{\mu A_p V^2}{8\pi^2 \quad X_L^2}$

Considering equations (29) and (33) we have the following equation:

$$\frac{dV}{dt} + \alpha V = \beta' \frac{I_{max}}{Z^2_{max}} \cdot e^{-\frac{R}{2L}t} \sin \omega t \quad . \quad . \quad (34)$$

where $\beta' = \frac{\mu A_p V}{8\pi^2 m_p X_L}$

The solution of (34) can proceed as follows:

$$\frac{d(Ve^{\alpha t})}{dt} = \beta' \frac{I_{max}}{Z^2_{max}} e^{(\alpha - \frac{R}{2L})t} \sin \omega t = \beta' \frac{I_{max}}{Z^2_{max}} e^{(\alpha - \frac{R}{2L} + \omega i)t} \quad . \quad . \quad (35)$$

where $e^{i\omega} = \cos \omega t + i \sin \omega t$ and $\sqrt{-1} = i$;

After integration we take only the imaginary part of the solution

Integrating (35) we obtain

$$Ve^{\alpha t} = \beta' \frac{I_{max}}{Z^2_{max}} \frac{e^{(\alpha - \frac{R}{2L} + \omega i)t}}{(\alpha - \frac{R}{2L} + \omega i)} + C$$

where C = constant of integration.

or

$$V = \beta' \frac{I_{max}}{Z^2_{max}} e^{-\alpha t} \left\{ \frac{\left[(\alpha - \frac{R}{2L}) \sin \omega t - \omega \cos \omega t\right] e^{(\alpha - \frac{R}{2L})t} + \omega}{(\alpha - \frac{R}{2L})^2 + \omega^2} \right\}$$

and
$$V = \frac{\beta' I_{max}}{Z^2_{max}\,\omega} e^{-\alpha t}\left\{\frac{\left[\left(a-\frac{R}{2L}\right)\big/_{\omega}\sin\omega t - \cos\omega t\right] e^{\left(\alpha-\frac{R}{2L}\right)t}}{\left(a-\frac{R}{2L}\right)^2\big/_{\omega^2}+1} + 1\right\} \quad (36)$$

Equation (36) can be written in dimensionless form as follows:

$$\frac{V Z^2_{max.}\,\omega}{\beta' I_{max}} = \frac{e^{-\alpha t}\left\{\left[\left(\frac{\alpha-\frac{R}{2L}}{\omega}\right)\sin\omega t - \cos\omega t\right] e^{\left(\alpha-\frac{R}{2L}\right)t} + 1\right\}}{\left(\frac{\alpha-\frac{R}{2L}}{\omega}\right)^2 + 1} \quad (37)$$

The parameter $\frac{V Z^2_{max}\,\omega}{I_{max}\,\beta'}$ is dimensionless; substituting for β' we obtain the following:

$$\bar{V} = \frac{V Z^2_{max}\,\omega}{I_{max.}\,\beta'} = \frac{8\pi^2 V Z^2_{max}\, m_p\, \omega^2 L}{I_{max.}\, V \mu\, A_p} \quad . \quad . \quad , \qquad (38)$$

Rewriting eq. (37) we have:

$$\bar{V} = \frac{e^{-\alpha t}\left\{\left(\frac{\alpha-\frac{R}{2L}}{\omega}\right)\tan\omega t - 1\right\}\cos\omega t\, e^{\left(\alpha-\frac{R}{2L}\right)t} + 1}{\left(\frac{\alpha-\frac{R}{2L}}{\omega}\right)^2 + 1} \qquad (37)$$

It was found previously that the resistance and inductance in the driver plate are given by:

$$R' = 2\mu r \frac{d \ln \bar{Z}}{dt}$$

and

$$L' = 2\mu r \ln \bar{Z}$$

During the initial stages $\bar{Z} \cong 1$ whereas $\frac{d\bar{Z}}{\bar{Z}\,dt}$ is a large number.

Thus, the reflected resistance dominates and the system is overdamped.

From test results (see Figures 1 & 2) it was deduced that for one particular case the system was overdamped, or near critically damped.

The equivalent to equation (37) can, in this case, be written as follows:

$$\bar{V} = \frac{V I_{max}^2 \cdot N}{\beta' I_{max}} = \frac{e^{-\alpha t}\left\{\left(\frac{\alpha-\frac{R}{2L}}{\omega}\right)\tanh Nt - 1\right\}\left\{\cosh \omega t\, e^{\left(\alpha-\frac{R}{2L}\right)t} + 1\right\}}{\left(\frac{\alpha-\frac{R}{2L}}{N}\right)^2 + 1} \quad \text{where: } N = \sqrt{\left(\frac{R}{24}\right)^2 - \frac{1}{CL}} \qquad (39)$$

Equations (37 and (39) provide a relationship between the plate velocity and time. The equation can be integrated again to give the plate displacement versus time relationship; this, however, is not necessary at this time.

From the momentum relationship of the wave in water, (i. e. $\rho_w C_w V$ = P where P is the pressure of the propagated wave), the analytical work can be compared with the experimental results.

A Kistler Pressure Transducer records the pressure versus time profile; the profile is then converted into a velocity versus time relationship. This relationship is then compared with the theoretical relationship given by Eq. (37) or (39).

In the preliminary work, equation (33) was solved graphically. Although it did not include the boundary conditions which were imposed later, the effects of insulation thickness, capacitor voltage, and damping were shown clearly. See Figures 7 and 8.

5.0 An Arithmetical Example

Using the test results as a guide, it is noted that the time to reach the peak current was 100 u sec., remembering that $\frac{dI}{dt}$ and $\frac{dI}{dt} = 0$ represents the point at which the driver plate is either completely uncoupled or coupled in the opposite direction.

Furthermore, if the system was overdamped, the time to reach peak current is given by $t_p = \frac{1}{N}$ where $N = \sqrt{\left(\frac{R}{2L}\right)^2 - \frac{1}{CL}}$

Therefore, $N' = \frac{\pi}{4 \times 100} \times 10^6 = 0.79 \times 10^4 \frac{1}{sec}$

Since neither L nor R are known, it is first assumed that $\frac{R}{2L} \simeq \sqrt{\frac{1}{CL}}$

Now, the inductance of the coil with the plates on either side is taken as **0.36** μ henry.

With $C = 960 \mu f$, $\frac{1}{CL} = 8.7 \times 10^8$: Therefore $\frac{R}{2L} = 9.3 \times 10^4 \frac{1}{sec}$

The value Nt is small enough to allow $\sinh N't \simeq N't$ and $\cosh N't \simeq 1$ also $\tan N't \simeq 1$. (the same result is found by considering $\sin \omega t \simeq \omega t$ and $\cos \omega t \simeq 1$)

Either equation (37 or (39) can be used.

Thus substituting in eq. (37) we obtain the following

$V = 369$ ft/sec $\quad t = 50 \mu sec$

$V = 262 \quad t = 30$

$V = 70 \quad t = 10$ $\qquad$ see Fig 3.

where the parameter $\frac{\gamma_{max}^2 N'}{\beta' I_{max}^2}$ was calculated as follows:

$$\frac{\beta' I_{max}}{\gamma_{max}^2 N'} = \frac{I_{max} V \mu A_p}{8 \pi^2 M_p N'^2 L \gamma_{max}^2} = 420 \frac{ft}{sec}$$

and

$I_{max} = 30{,}000$ amp

$V = 11 \times 10^3$ volts

$\mu = 4\pi \times 10^{-7}$ henry/m

$A_p = 113$ in^2

$m_p = 11.4$ lb

$L = 0.12\ \mu$ henry*

$z_{max} = 0.07$ in.

$z_0 = 0.05$ (separation between coil and plate)

N. B. 1. from the preliminary solution given in the last monthly report, it was found that the plate moves only a few thousanths for all the cases, during time t_p

When $\frac{dI}{dt} = 0$, it was found that $\frac{dz}{dt}$ must reverse: this indicates that the plate is no longer repulsed but instead it is attracted towards the coil. The plate, however, cannot reverse instantaneously, because it has forward momentum. Thus while V is decreasing, it is nevertheless positive**

Thus, the induced voltage is considerably reduced.

(i. e. $V = -2\mu \frac{r}{z} \cdot \frac{dz}{dt} - 2\mu r \ln z \frac{dI}{dt}$). The plate therefore decelerates under the opposing force $\propto V$. More precisely we have the following:

$$\frac{dV}{dt} + \alpha V = 0 \quad . \quad . \quad . \quad . \quad . \qquad (40)$$

and $V = C e^{-\alpha t}$

where, $C = V_{max} e^{\alpha t_p}$

Therefore $$\frac{V}{V_{max}} = e^{-\alpha(t - t_p)} \quad . \quad . \quad . \qquad (41)$$

* The inductance L, is the total inductance of the system; more details will be given in the next monthly report.

** It must be noted here that $\frac{dz}{dt}$ is no longer identified with the velocity of the plate when uncoupling has taken place.

The deceleration, however, may be assisted by some attraction from the coil: this is indicated in the tests. Alternately, if coupling in the opposite direction is the dominating force then the declerating phase is governed by the same equations as in the accelerating phase with $\frac{d\dot{x}}{dt}$ negative and the boundary conditions $V = V_{max}$ at $t = t_p$ and

$V = 0$ at the end of the pulse.

The energy under the wave pulse is equal to approximately 1500 joules.* The energy stored in the bank was 58,000 joules. This will indicate that the coil is only 2.6% efficient.

In the analysis, however, it is shown that the pulse is short, because of the reversal of the current: thus, the energy delivered to the plate is inherently dependent on the characteristics of the particular energy source.

By contrast this dependence does not exist in the EBW effect since the current cut-off is associated with the explosive backward voltage of $\frac{dI}{dt}$ In the E. B. W., the size of the wire can also change the cut-off time. In the transducer, attempts can be made whereby a change of the source characteristics can extend the positive $\frac{dI}{dt}$ and thereby increase the energy delivered to the coil.

The coupling is at present estimated to be 50-70%. More details, however will be given in the next monthly report.

In summary, there are indications that coupling of the coil to the driver is better than E. B. W., but its efficiency, based on the characteristics of the bank described previously, is considerably lower. In addition the energy delivered to the plate is uni-directional and therefore more controllable than the E. B. W.

To improve on the efficiency, it is necessary to consider the transducer with the capacitor bank that it is connected with. There is quite a difference in the results between the 960 uf and 240 uf bank. (see Figs. 4, 5, 6)

6.0 Other Activity

It was found that using a pancake coil has definite electrical advantages

* $\text{ENERGY} = \frac{A_P}{C_w \rho_w} \int P^2 dt$

but it presents a serious problem structurally. Coils with different epoxies and fiberglass re-inforcements were made and tested. There are indications that the 12" pancake coil cannot withstand "delivered energies" more than 2000 joules. The requirement of minimum separation between plate and coil does not allow a buildup of re-inforced epoxy on either face of the coil. From the results of the analogue computer shown in last months report, the separation distance is a very important parameter because it affects the magnetic pressure as the inverse of its square. (i. e. $\frac{B_x^2}{2r} \propto \frac{1}{x^2}$) In the tests this was indeed found to be important. A good compromise was found at 0.05 in. in the front face and 0. 125 in the rear.

Two methods were used. a) the coil was free to follow the driver plate vertically and b) the coil was held on its periphery. In both cases the coil was placed between the aluminum plate and the bottom driver plate. See Fig's. 4, 5, 6.

While other tests were made, the generated wave has been used to form a 28 inch dome. There are indications that higher wave pressures than those used so far are required to form the final stages of the dome.

In all the tests a Kistler pressure transducer 617L was used to sense the wave pressure.

In case (b), there is vacuum created between the coil and the driver plate, during the discharge, which pulls back and re-positions the driver plate at the end of the cycle. This allows the frequency of applications to be as high as one every 5 seconds. It must be done with caution, however, because if the plate is not pulled back in place, the coil will be blown out in the following discharge under the influence of the top plate. A mechanism to check the re-position will soon be installed.

In summary, a pancake coil was built and tested with 58,000 joules at 960 uf and with 23,000 joules at 240 uf. The coil is located between two aluminum plates one of which is free to move against a water column vertically, and the other against a column of rubber pads. (see Fig. 6). Furthermore the coil is held at its periphery. The driver plate is re-positioned by the vacuum created between the coil and the plate. Pressure records with 617L Kistler gauge were taken.

Anticipated work during January 1 to February 1

1.0 More examples will be worked out theoretically: the results will be compared with test results. In these runs other parameters, (i.e. plate weight, separation distance, coil turns) will be varied.

2.0 Attempts to design a structurally stronger 12" coil will be made.

3.0 Attempts to form a 28" dome completely will also be made.

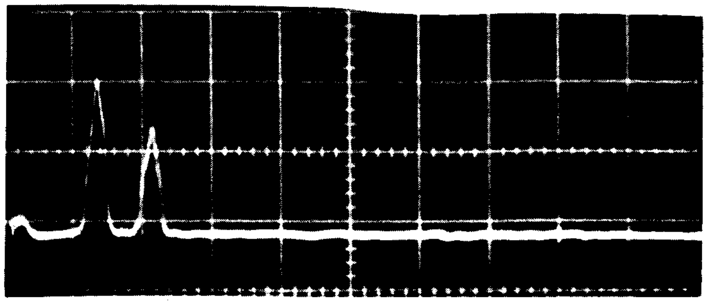

Capacitor Bank: 11 KV, 960 uf, 58,000 Joules

0.2 m sec/cm   38, psi/cm

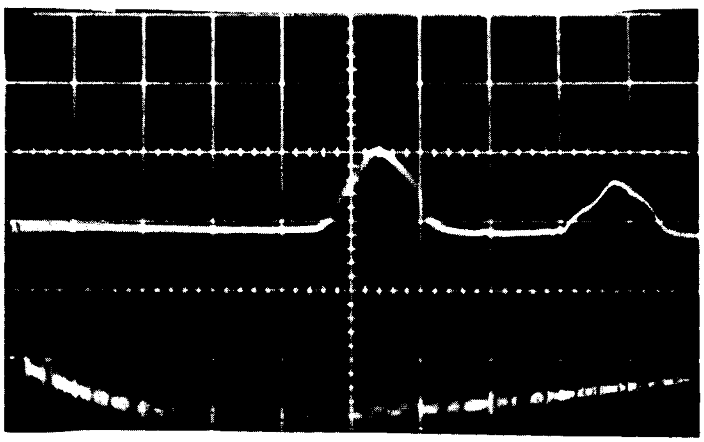

Capacitor Bank: 11 KV 960 uf, 58,000 Joules

50 u sec/cm   7700 psi/cm

ELECTROMAGNETIC TRANSDUCER PRESSURE RECORDS
FIGURE 1

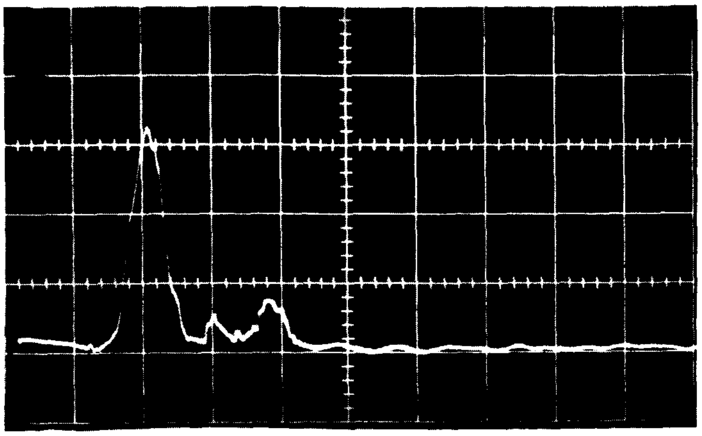

Capacitor Bank 14 KV, 240 uf, 23,520 Joules
0. 1 m sec/cm, 1540 psi/cm

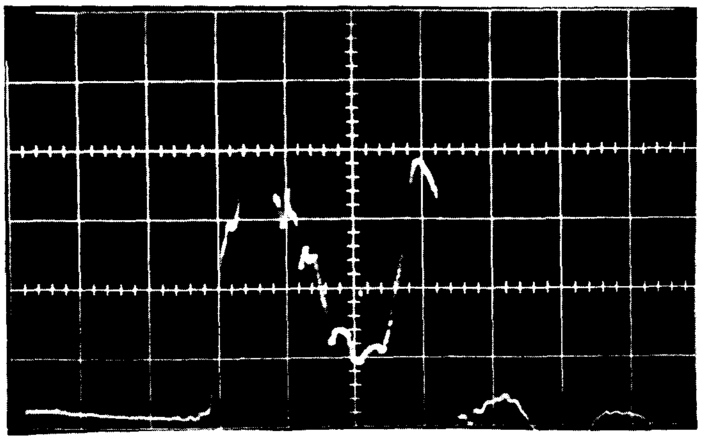

Capacitor bank: 14 KV, 240 uf, 23,520 Joules
50 u sec/cm 770 psi/cm

ELECTROMAGNETIC TRANSDUCER PRESSURE RECORDS
FIGURE 2

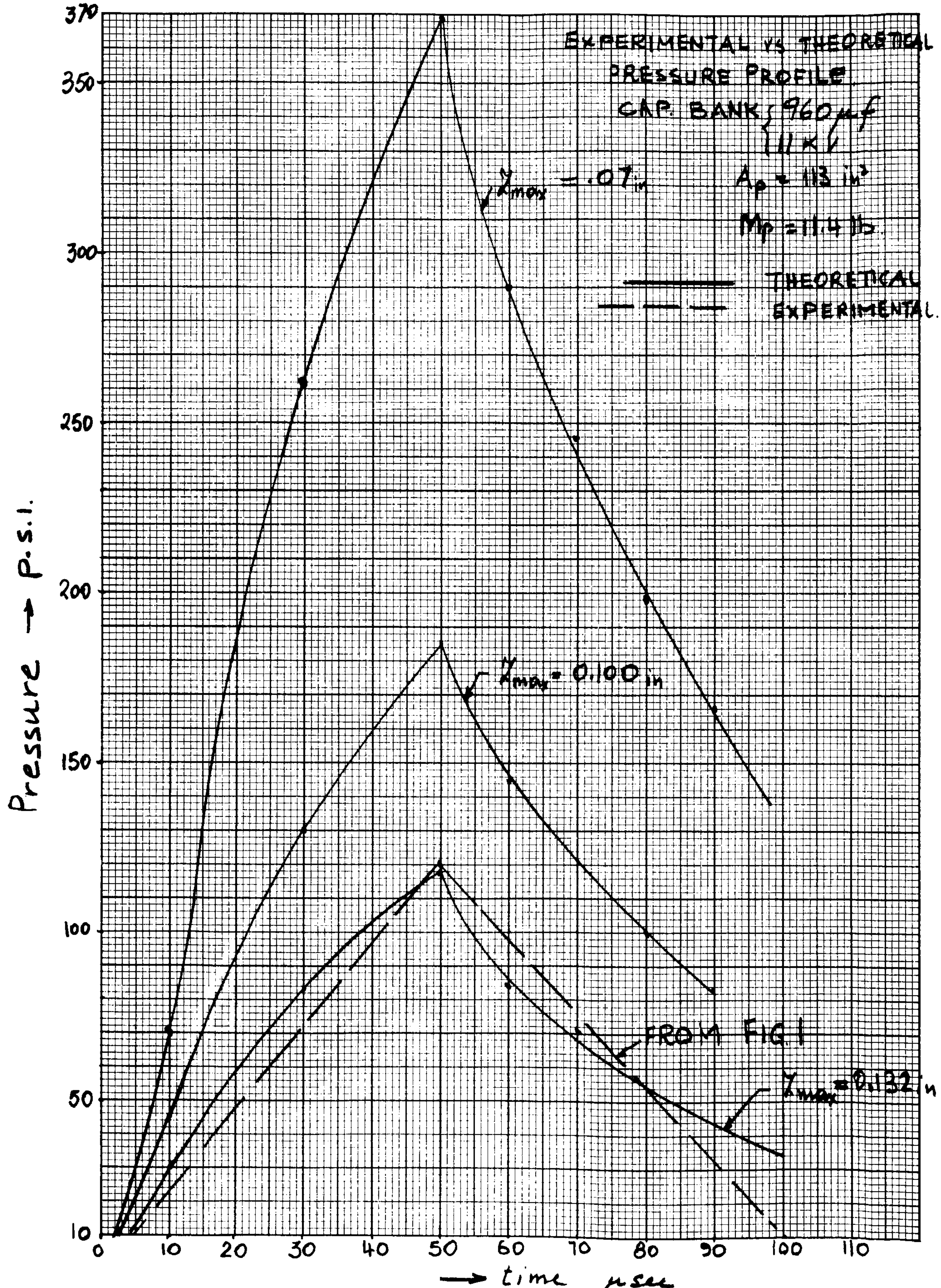

EXPERIMENTAL vs THEORETICAL PRESSURE PROFILE
CAP. BANK { 960 μf 11 kV
A_p = 113 in²
M_p = 11.4 lb
THEORETICAL
EXPERIMENTAL.
Z_{max} = .07 in
Z_{max} = 0.100 in
FROM FIG. 1
Z_{max} = 0.132 in
Pressure → p.s.i.
→ time μsec.
370
350
300
250
200
150
100
50
10
0
10
20
30
40
50
60
70
80
90
100
110

FIG 3

Case b) - The coil is held on its periphery

12" PANCAKE COIL. 21 TURNS

Insulation thickness: Front = 0.05 in.
Rear = 0.100 in.

FIGURE 4

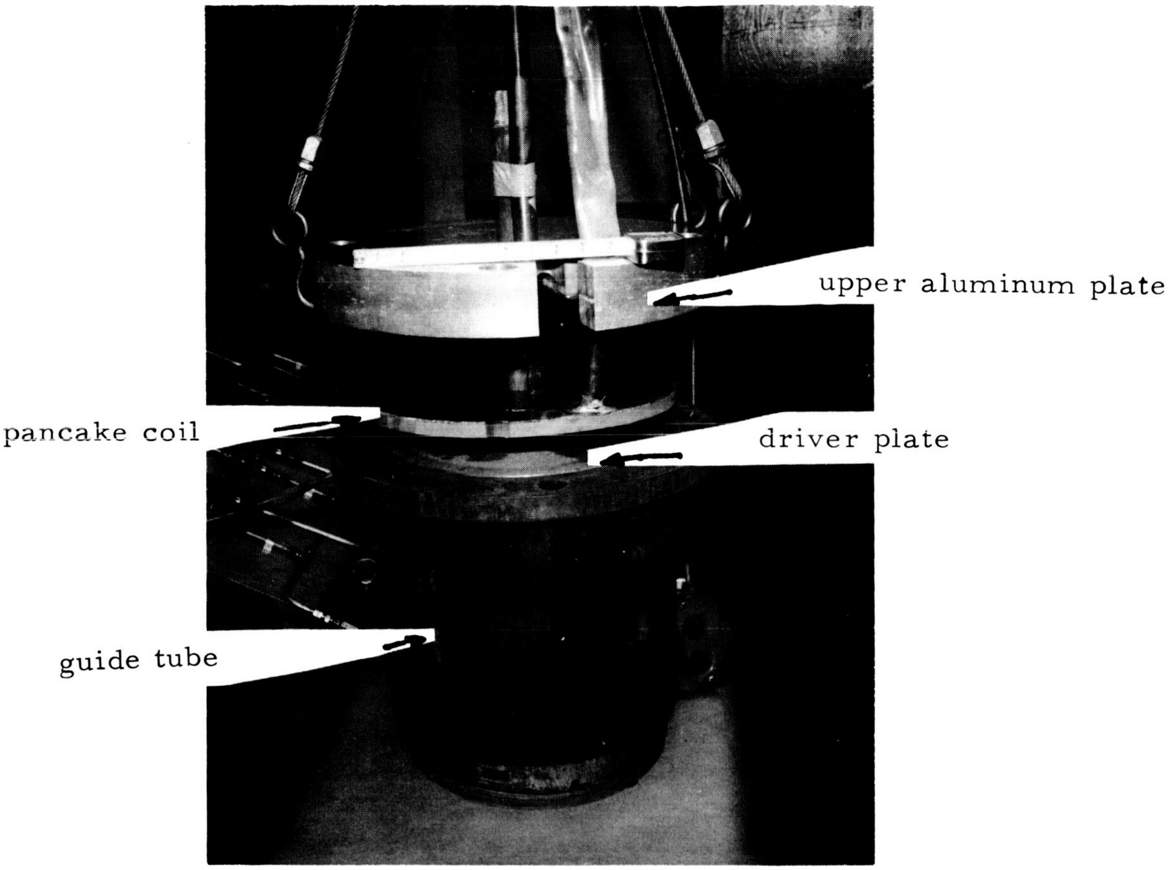

Case b) - The coil is held on its periphery

PANCAKE COIL ASSEMBLY
FIGURE 5

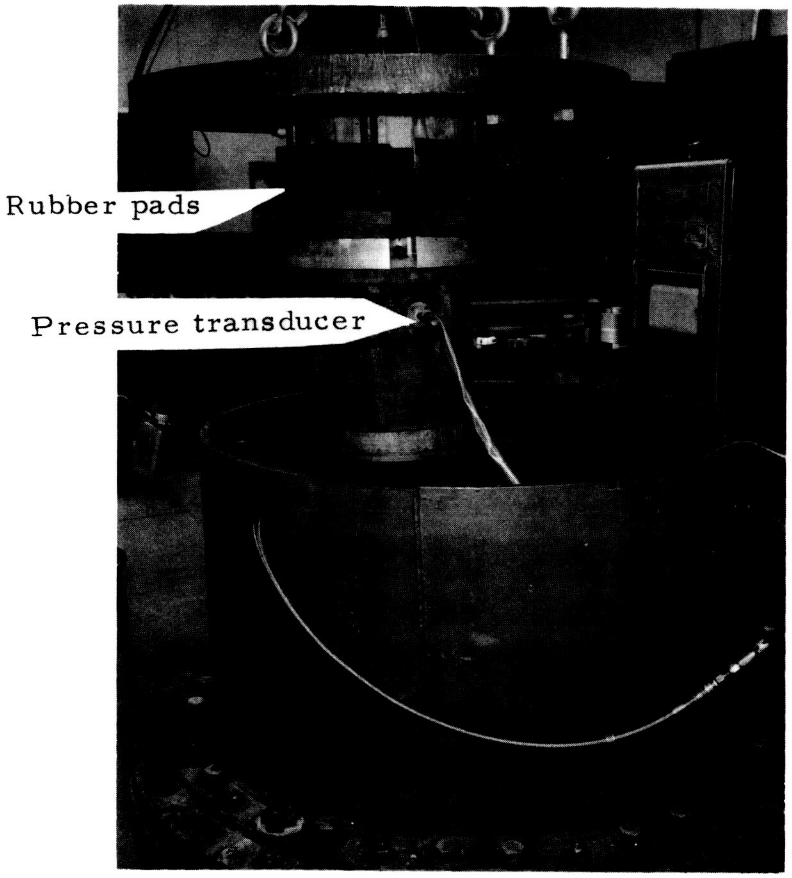

Case b) - The coil is held on its periphery

ELECTROMAGNETIC WAVE GENERATOR
FIGURE 6

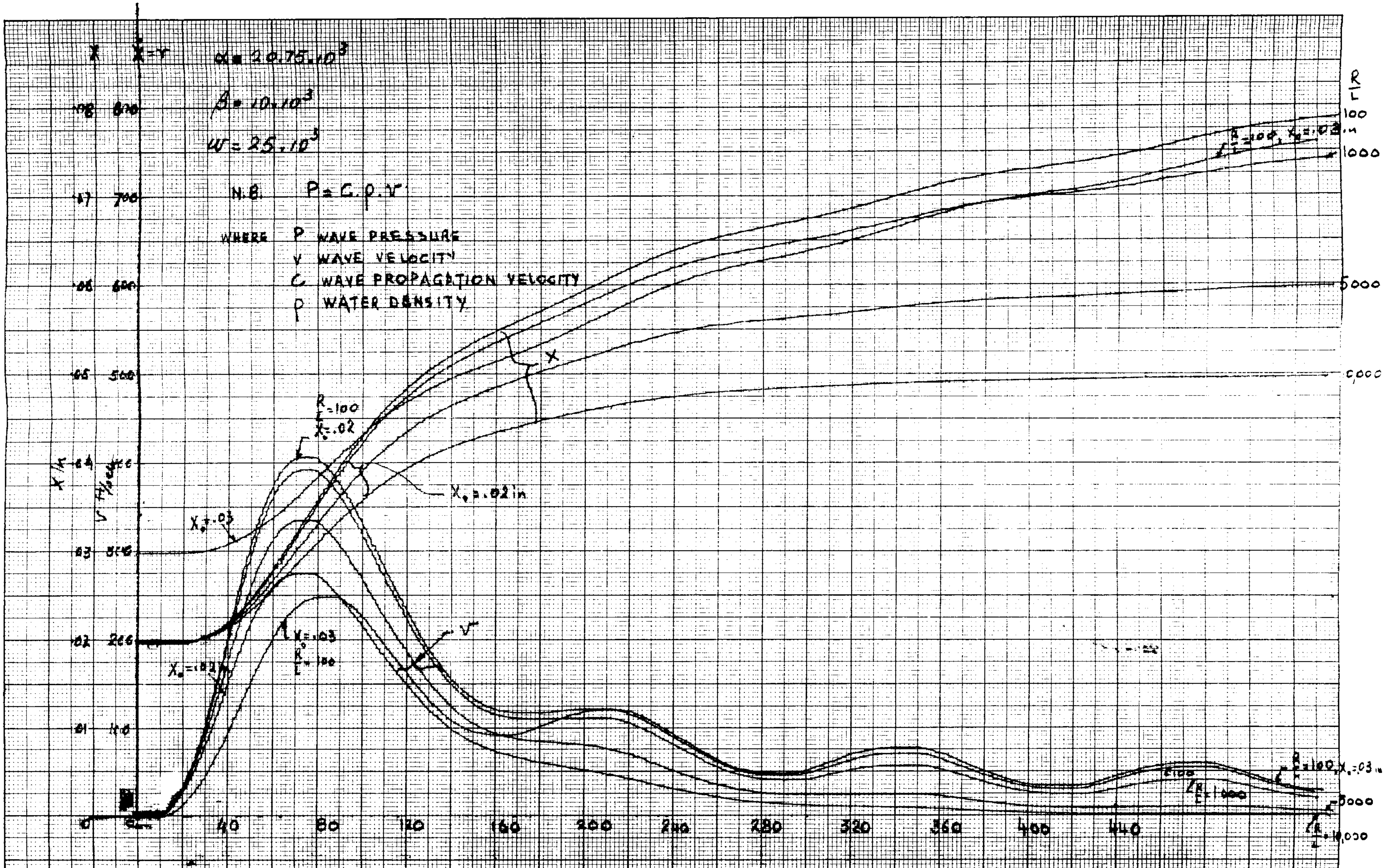

GRAPHICAL SOLUTION OF EQU. 38

FIG 7